

# Adjusting Stereoscopic Parameters by Evaluating the Point of Regard in a Virtual Environment

## Abstract

Despite the growth in research and development in the area of virtual reality over the past few years, virtual worlds do not yet convey a feeling of presence that matches reality. This is particularly due to the difference in visual perception of flat images as compared to actual 3D. We studied the impact of two parameters of the stereoscopic configuration, namely, the inter-camera distance (ICD) and the presence of a depth of field blur (DOF blur). We conducted an experiment involving 18 participants in order to evaluate this impact, based on both subjective and objective criteria. We examined six configurations which differed in the presence or absence of DOF blur and the value of the ICD: fixed and equal to the anatomical interpupillary distance, fixed and chosen by the participant, or variable, depending on the depth of the viewer's point of regard (POR). The DOF blur and variable ICD require the use of an eye tracking system in order to be adjusted with respect to the POR. To our knowledge, no previously published research has tested a gaze-contingent variable ICD along with dynamic DOF blur in a Cave Automatic Virtual Environment. Our results show that the anatomical and variable ICD performed similarly regarding each criterion of the experiment, both being more efficient than the fixed ICD. Besides, as with earlier similar attempts, the configurations with DOF blur obtained lower subjective evaluations. Although mainly not significant, the results obtained by the variable ICD and DOF blur are likely due to a noticeable delay in the parameters update. We also designed a new methodology to objectively compare the geometry and depth rendering, based on the reproduction of the same scene in the real and virtual setups, and then on the study of resulting ocular convergence and angular deviation from a target. This leads to a new comparative criterion for the perceptual realism of immersive virtual environments based on the visual behavior similarity between real and virtual setups.

*Keywords:* Virtual reality, Stereoscopic parameters, Inter-camera distance, Depth of field blur, Point of regard tracking

## 1. Introduction

Because of its immersive nature [1], virtual reality (VR) is a powerful tool with many applications, ranging from entertainment to more practical uses, such as training through simulations or in medical practice. These practical applications do however call for a strong sense of immersion and perceptual realism<sup>1</sup>, in order to bring the behaviors expressed during an immersive experience as close as possible to those seen in a real setup. For example, clinical research in psychiatry used ocular behavior in VR in order to assess phobic avoidance or sexual preferences [2][1][3]. Expressing the same behaviors in immersion as in real life could thus enhance the validity of such an assessment procedure, and the use of virtual environments and avatars instead of real scenes and people. VR is often used in combination with stereoscopic displays, which can intensify the feeling of immersion [4].

Immersion in a stereoscopic environment can be visually constraining, particularly due to a conflict between accommodation (adjustment of the eye lenses to focus at the observed depth) and eye convergence. While these two phenomena are cross-linked in normal viewing conditions, in a Cave Automatic

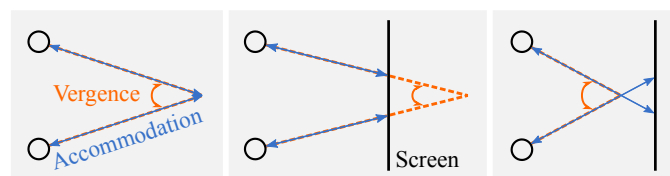


Figure 1: (Left) Cross-link between accommodation and vergence angle in normal viewing conditions. (Middle and right) In virtual environments, a conflict arises between the amount of accommodation and the vergence angle

<sup>1</sup>In the scope of this article, we do not designate by perceptual realism the graphical realism, mainly provided by the shapes and textures of the elements of the virtual environment, but the closeness between the viewer's perception of the virtual environment and an identical real one.

Virtual Environment (CAVE) the viewer always focuses at the screen level regardless of the vergence angle, which leads to a conflict [5][6][7][8] as can be seen on Fig. 1. Lambooj et al. [7] cite as other common causes of visual fatigue: rapid vergence movements that stress this conflict, excessive binocular parallax (leading to diplopia), and unnatural blur intensities (causing ambiguous or erroneous depth perception).

Stereoscopic parameters play an important role in visual comfort. First, linked parameters (cameras' orientation relative to each other and distance between them, see Fig. 2 (top left)) will impact the disparity between left and right images, and thus influence the amount of perceived depth [9], as well as visual comfort. Nevertheless, there is no single optimal inter-camera distance (ICD) setting that minimizes the fusion effort and leads to optimized depth perception for varying viewing circumstances and depth ranges [10]. Indeed, the incidence of

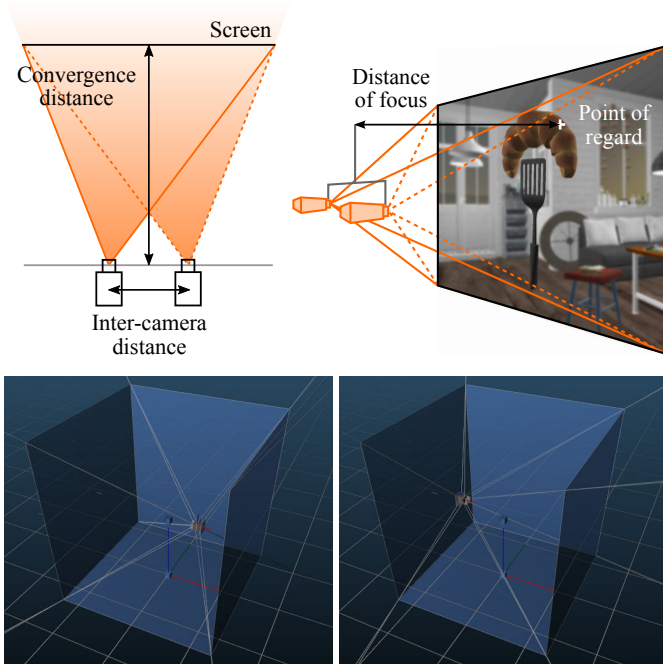


Figure 2: (Top left) In a typical CAVE environment, cameras are parallel with asymmetric view frustums. The distance of convergence used is the one between the viewer and the screen. (Top right) The distance of focus is used to adjust the DOF blur. (Bottom) Dynamic frustums adjustment to the position of the viewer’s head

67 system we use provides sight directions and vergence informa-  
 68 tion, which allow us to link objective measurements to the real-  
 69 ism of the geometry rendering of the scene (depths, positions,  
 70 relative distances and sizes). To the best of our knowledge, pre-  
 71 vious experiments dealing with ocular movements induced by  
 72 VR were only based on qualitative considerations [12][13][14].  
 73 We thus designed an innovative test that compares eye move-  
 74 ments while viewing a real scene and its virtual copy. The ver-  
 75 gence similarity, which can be quantified, provides indications  
 76 as to whether the depth is perceived similarly in both virtual  
 77 and real cases, and whether the ocular behavior of the viewer  
 78 remains the same. Our main contributions can be summarized  
 79 as follows: (1) we investigate a new value for ICD which varies  
 80 in real time with respect to the POR and the user’s choices; (2)  
 81 we evaluate six stereoscopic configurations in an experiment in-  
 82 volving 18 participants, and (3) we design a new methodology  
 83 to quantify and compare simulation realism.

## 84 2. Related Work

85 Although many papers have covered stereoscopic param-  
 86 eters involved in VR quality, we did not find a study that com-  
 87 bines adjusted ICD according to the POR depth with an inter-  
 88 active DOF blur. This paper builds upon the following areas  
 89 of previous research: (1) stereoscopic parameters adjustment,  
 90 (2) methods for estimating the 3D POR, and (3) evaluation cri-  
 91 teria to compare stereoscopic configurations.

92 Regarding the configuration of the cameras system, we used  
 93 the typical setup of a CAVE, i.e. parallel cameras with asym-  
 94 metric frustum as presented in Fig. 2. The image-shifted and  
 95 converged system configurations are out of scope of the param-  
 96 eters we investigated in our approach, we refer the reader to  
 97 [15][16][17] for analysis using these configurations.

### 98 2.1. Inter-camera Distance

99 When dealing with immersion quality, the ICD is the first  
 100 factor that comes out as it strongly impacts both visual com-  
 101 fort and depth perception. In the experiment of Best [18], ICD  
 102 values of 5.0 cm and 7.4 cm significantly increased visual fa-  
 103 tigue compared to 6.3 cm, which is the average adult IPD. In-  
 104 deed, an ICD value too high results in an excessive binocu-  
 105 lar parallax that notably leads to eye-straining visual artifacts  
 106 like diplopia [7]. Moreover, inadequate ICD values lead to an  
 107 under- or over-estimation of depth judgment [10].

108 Using an ICD different from the IPD seems to be contradic-  
 109 tory with the search of realism in the depth and distance ren-  
 110 dering, as it implies a space deformation. However, “disparity  
 111 depth cue is a highly flexible depth enhancement, rather than  
 112 the primary determinant of 3D space perception” [19], as other  
 113 depth cues intervene in the brain’s processing of the stereo-  
 114 scopic images. Ware [19] noted that his participants could com-  
 115 fortably work with ICD larger than their IPD, and suggests that  
 116 it might not be mandatory to make both values match.

38 ICD is intrinsically linked to the interpupillary distance (IPD)  
 39 of each individual [7]. The known methods to choose the best  
 40 possible ICD value will be developed in Sec. 2.1. We decided to  
 41 investigate an approach still unexplored which brings together  
 42 several solutions, namely, the variable ICD. It adapts the ICD  
 43 in real time based on the current sampled depth, given by the  
 44 3D point of regard (POR), and the viewer’s preferences, as ICD  
 45 will linearly vary between three values chosen by the viewer for  
 46 three predetermined POR depths.

47 We also used the POR in order to adapt a second param-  
 48 eter: a depth of field blur (DOF blur) that simulates the one  
 49 that occurs in natural vision due to the accommodation phe-  
 50 nomenon. In a CAVE, this physiological blur is not correlated  
 51 to the distance of the observed object as the eyes always focus  
 52 at the screen level. Moreover, adding a synthetic DOF blur re-  
 53 quires to monitor the POR in order to adapt the blur location  
 54 accordingly (see Fig. 2 (top right)). When blur is not added to  
 55 an immersive system, the resulting images are unnatural with  
 56 only sharp objects. While it is true that DOF blur has already  
 57 been studied in other papers, Hillaire et al. [11] emphasize the  
 58 fact that the processing capacity was only recently acquired to  
 59 compute this interactive blur in real time, and that we still need  
 60 to evaluate its impact on viewers’ performance and subjective  
 61 preferences. We hypothesized that by leading the virtual scene  
 62 perception closer to reality, blur could increase the feeling of  
 63 immersion.

64 Finally, we were interested in quantifying the perceptual re-  
 65 alism of the simulation, not only based on subjective evalua-  
 66 tions, but also on objective criteria. The binocular eye tracking

### 117 2.1.1. Fixed ICD

118 If the ICD value is fixed, it is often determined after sev-  
119 eral attempts by the scene creator and used as is for every  
120 viewer, which only ensures that stereoscopic images suit the  
121 creator’s binocular vision [9]. The viewer may also be allowed  
122 to choose, thus taking into account his subjective preferences  
123 and indirectly considering his anatomical IPD. Nevertheless,  
124 Wann et al. [14] noticed that their participants adjusted the ICD  
125 so that images merge where their eyes did converge, “regardless  
126 of the apparent location within the virtual world”. Furthermore,  
127 the ICD chosen was systematically smaller than the anatomical  
128 IPD. Finally, the ICD can be fixed according to the depth inter-  
129 val the viewer would need to sample, as recommended by Wann  
130 et al. [14]. According to them, at a close working distance, an  
131 ICD which reduces fusion effort is significantly smaller than the  
132 IPD.

133 However, using a fixed ICD is tantamount to assuming that  
134 the viewer’s vergence remains constant, that is, the depth sam-  
135 pled in the scene is fixed [14]. Since that is generally not the  
136 case, a dynamic adjustment is therefore needed.

### 137 2.1.2. Dynamic Adjustment

138 The ICD value can be modified in real time depending on  
139 the viewer’s position and movements, the task he has to per-  
140 form, where he is looking at, or just so that the disparities val-  
141 ues stay more comfortable. The ICD adjustment can be com-  
142 bined with a modification of the scene such as scaling. Jones  
143 et al. [9] described a method for the real-time calculation of the  
144 positions of the virtual cameras that minimize distortions as the  
145 viewer’s head moves. They diverged from the current notion  
146 that cameras must follow eye positions, and instead used a pro-  
147 portional relationship when head movements are parallel to the  
148 screen. They also used a method of Depth Range Control that  
149 maintains a fixed perceived depth distribution when the viewer  
150 moves towards or away from the screen.

151 It is worth noting that ICD dynamic adjustment is not neces-  
152 sarily aimed at searching for perceptual realism, it may also be  
153 used to only enhance depth perception [10] or increase visual  
154 comfort. For instance, Ware [19] artificially scaled the scene  
155 in order to optimize disparities for depth discrimination and to  
156 reduce visual discomfort due to the accommodation-vergence  
157 conflict. These adjustments force the viewer to adapt his depth  
158 judgments continuously, in particular when size cues remain  
159 unchanged while depth cues vary [10]. However, given that  
160 depth perception is dominated by other cues such as motion  
161 parallax, the ICD changes can remain unnoticed, especially if  
162 they occur gradually over a few seconds [19].

163 In our research, for the purpose of increasing perceptual re-  
164 alism, we test the adjustment of the ICD as a function of the  
165 position of the POR. Wann et al. [14] argue that the ICD should  
166 vary at the same time as the vergence angle, as the latter in-  
167 troduces small changes in the IPD due to the eye rotation cen-  
168 ters located 5-6 mm behind the nodal point of the optical sys-  
169 tem [20]. For example, the IPD decreases by 1 mm between  
170 focal distances at infinity and at 30 cm, leading the viewer to  
171 perceive depth differently. Several related works that adapted  
172 the ICD to the viewer’s POR improved the performance of the

173 stereoscopic configuration. Celikkan et al. [21] obtained better  
174 ratings in terms of perceived depth, visual comfort and image  
175 quality with their technique of Dynamic Attention-Aware Dis-  
176 parity Control. Yet, they did not use eye tracking, but rather es-  
177 timated the POR based on a scene content analysis. Kulshreshth  
178 and LaViola Jr [22] also proposed a POR-contingent algorithm  
179 that dynamically adjusts ICD and convergence distance to pro-  
180 jection surface. Their results on depth judgment tasks indicate  
181 that the adjusted parameters provide enhanced depth percep-  
182 tion compared to fixed parameters, even in scenes with an ob-  
183 ject close to the camera. Finally, Bernhard et al. [23] found that  
184 gaze-controlled adjustment can “lower fusion time for large dis-  
185 parities”, the fusion time being used as a discomfort measure-  
186 ment. In addition, they recommend to apply this adjustment  
187 in a personalized manner. This is what we aim to do in our ap-  
188 proach, by letting the participant choose three ICD values while  
189 observing objects at three predefined depths. The ICD will then  
190 be computed in real time based on the POR, by means of a  
191 linear interpolation between these three values, which, to our  
192 knowledge, is a solution that has never been tested in a CAVE.

### 193 2.2. Depth of Field Blur Influence

194 The second parameter we investigate in order to improve  
195 the configuration quality is the simulation of a DOF blur. We  
196 assume that the DOF blur can increase perceptual realism and  
197 depth perception as accommodation blur is used by the brain in  
198 normal vision as a depth clue [11].

199 In a non-stereoscopic experiment, Hillaire et al. [24] com-  
200 pared three conditions of navigation: (1) without blur, (2) with  
201 blur computed considering that the POR stays in a centered  
202 rectangular area, and (3) with blur computed using eye track-  
203 ing. The first two conditions obtained similar results, but the  
204 last one was significantly better in terms of fun and immer-  
205 sion. Other researches suggest that blur can significantly re-  
206 duce visual fatigue [6][25] or discomfort [26]. Indeed, even  
207 if it does not stimulate accommodation, it might alleviate the  
208 accommodation-vergence conflict by producing a “natural re-  
209 lationship between retinal image blur and binocular disparity”,  
210 as well as enhance depth perception [5]. Also, Nagata [27] ob-  
211 served that a blurred background increased the limits of fusion,  
212 i.e. the depth range for which stereoscopic images can be fused  
213 without experiencing diplopia, although their experiment only  
214 involved three participants. This is likely due to the fact that  
215 “the limits of fusion increase as a result of the decreased spatial  
216 frequency” in natural vision [7].

217 However, other related works show more mixed results. An-  
218 other non-stereoscopic study by Hillaire et al. [11] revealed that  
219 blur had a significant negative effect on the performance, and no  
220 effect on the subjective evaluation of realism, fun, perception of  
221 depths and distances, and feeling of immersion. However, they  
222 did not use an eye tracking system, and the blur appeared dis-  
223 turbing when participants explored the image outside the area  
224 where the POR was assumed to stay. For the stereoscopic case,  
225 the experiment of Brooker and Sharkey [28] did not reveal per-  
226 formance improvement when the blur is computed using eye  
227 tracking. Vinnikov and Allison [5] also reported that adding a  
228 dynamic DOF in stereoscopic conditions did not enhance depth



Figure 3: Corneal reflections of infrared emitting diodes

229 impressions and reduced image quality and viewing comfort.  
 230 Finally, the participants of Duchowski et al. [26] expressed a  
 231 non-significant dislike towards DOF blur. These poor results  
 232 are generally likely attributed to the noticeable delay in DOF  
 233 update, Duchowski et al. [26] adding the spatial inaccuracy of  
 234 the eye tracker. Brooker and Sharkey [28] suggested to further  
 235 evaluate the real-time DOF blur effect in a virtual environment,  
 236 which is one of the objectives of our study.

### 237 2.3. Point of Regard 3D Position

238 In typical eye tracking systems, sight directions are de-  
 239 termined using the geometric relationship between the center  
 240 of the pupil and corneal reflections [29] produced by infrared  
 241 emitting diodes (see Fig. 3). However, in order to get the  
 242 3D POR, the depth along these directions must be determined.  
 243 This requires greater technical effort [30], for example, using a  
 244 binocular system, as in the methods reviewed below.

#### 245 2.3.1. Inferring from Vergence Movements

246 This category of techniques takes advantage of the fact that  
 247 the POR depth variation is accompanied by an ocular conver-  
 248 gence movement. The vergence angle varies from about  $14^\circ$   
 249 when the POR moves from infinity to a distance of about 25 cm,  
 250 which is “the nearest distance for comfortable convergence”,  
 251 and from about  $36^\circ$  when it moves to the closest convergence  
 252 point [13]. Nearly 70% of the vergence angular variation occurs  
 253 within a range of 1 m. Moreover, it has been shown that stereo-  
 254 scopic stimuli induce adequate convergence movements despite  
 255 accommodation-vergence conflict [13][12][14], lending legiti-  
 256 macy to this method even in virtual environments. However,  
 257 due to the noise level in raw eye tracking data and the nonlinear  
 258 relationship between the vergence angle and the POR depth, its  
 259 accuracy remains poor. For example, Daugherty et al. [13] mea-  
 260 sured the vergence angle while displaying a target on a plane at  
 261 three increasing depths. They obtained a higher angle for the  
 262 back plane than for the middle one (respectively around 0.82  
 263 for the front, 0.26 for the middle, and 0.30 for the back after  
 264 normalization). Duchowski et al. [12], who used the vergence  
 265 angle to compute the POR depth, had to apply a filter and a  
 266 least squares fit in order to counter the significant noise level, as  
 267 well as wrong depth judgments by the participants. They even  
 268 noticed significant errors in the monoscopic case, with their es-  
 269 timated average depth not being located at the screen level, but  
 270 between 10 cm and 20 cm in front of it.

271 A similar idea consists in estimating the POR depth by eval-  
 272 uating the distance between pupil centers. Kwon et al. [29]  
 273 tested this approach for a gaze-dependent application, i.e. an

274 application in which interactions with virtual objects are made  
 275 through glances. They obtained a good accuracy, with 95.7% of  
 276 successful object selection over 30 trials, but their targets were  
 277 placed in a discrete partition of the virtual space. Indeed, due  
 278 to the noise level, the techniques based on vergence movements  
 279 are more adapted to scenes composed of discrete depth levels  
 280 than to rich environments. They also noted experimentally that  
 281 the function of theoretical variations  $f(IPD) = depth$  is not lin-  
 282 ear, making it necessary to rely on a calibration phase to define  
 283 the IPD range for each plane, for each participant.

#### 284 2.3.2. Intersection of Lines of Sight

285 A geometric approach consists in considering that the POR  
 286 is located at the intersection of the two lines of sight, or at  
 287 the closest point to both of them. Again, errors and noise  
 288 in the estimation of sight directions strongly impact the accu-  
 289 racy. To improve this estimation, Essig et al. [31] developed a  
 290 calibration method based on a Parameterized Self-Organizing  
 291 Map (PSOM), which is a type of artificial neural network. The  
 292 PSOM is trained in the calibration phase during which the par-  
 293 ticipants look at 27 markers. Then, during the test phase, the  
 294 PSOM corrects the measured sight vectors while the partici-  
 295 pants gaze at 16 markers. The distance between the estimated  
 296 POR and the actual marker position gives the accuracy mea-  
 297 surement. They obtained a global average error of 2.78 cm,  
 298 noting that most of the error is observed for the z-coordinate  
 299 (respectively 0.52 cm, 0.82 cm, and 2.53 cm, for x, y and z),  
 300 which highlights the fact that the depth information is the most  
 301 difficult to estimate.

#### 302 2.3.3. Intersection with Scene Geometry

303 Finally, the 3D POR can be determined by intersecting one  
 304 or both lines of sight with the virtual scene, the assumption  
 305 being that the first object intersected is the object of atten-  
 306 tion [30]. This requires knowledge of the scene geometry (as  
 307 is the case in virtual environments) and that sight directions  
 308 and eye positions be expressed in virtual world coordinates, by  
 309 combining eye tracking with head tracking and a calibration  
 310 phase. Pfeiffer [30] listed some limitations of this method, such  
 311 as when the target object for one eye is hidden by an element  
 312 in the view of the other eye. On the other hand, he underlines  
 313 its advantages, with the most important being that the POR  
 314 estimation obtained is fairly accurate.

315 Thus, while a significant variety of techniques were investi-  
 316 gated to obtain the 3D POR, many of them were unfortunately  
 317 proven to be inaccurate in the presence of the current level of  
 318 noise in eye tracking data. After an unsatisfactory attempt at  
 319 intersecting the lines of sight, we therefore decided to base our  
 320 approach on intersecting the scene geometry.

### 322 2.4. Comparative Criteria

323 Finally, we review the most common criteria used to com-  
 324 pare stereoscopic configurations.

### 325 2.4.1. Subjective Evaluations

326 In several research works [22][21][32][11], the authors  
327 asked their participants to grade each experimental configura-  
328 tion on various criteria using a 5-point or a 7-point Likert scale,  
329 from “bad” to “excellent”. Blum et al. [32] however allowed  
330 the participants to place their mark at any location, then mea-  
331 sured and converted the results to a scale between 0 and 100.  
332 In a similar way, we used a 7-point Likert scale ranged from  
333 “very negative” to “very positive”, then converted the marks  
334 to a scale between 0 and 1. Regarding the criteria, apart from  
335 the “visual comfort” which has been discussed in Sec. 2.1 and  
336 Sec. 2.2, we used the categories of “realism”, “fun”, “percep-  
337 tion of depths and distances”, and “feeling of immersion” used  
338 by Hillaire et al. [11].

### 339 2.4.2. Limits of Fusion

340 We designate as limits of fusion the distance between the  
341 viewer and the POR below which stereoscopic images cannot  
342 be merged. This happens when the parallax becomes excessive  
343 probably because of the too great dissociation between accom-  
344 modation and convergence [8][17]. This distance shall not be  
345 confused with the limits of Panum’s fusional area [6][7], which  
346 also contribute to fusion range but represent the distance be-  
347 tween the horopter and the boundaries of Panum’s area. We  
348 used the limits of fusion as another criterion linked to visual  
349 comfort. Indeed, the larger the depth range of easy fusion, the  
350 larger the variety of scenes that can be displayed while avoiding  
351 discomfort due to diplopia.

352 Jones et al. [9] reported an experiment in which the lim-  
353 its of fusion for a simple scene were generally located between  
354 30 cm and 50 cm in front of the screen, and between 2 m and  
355 20 m beyond it. Woods et al. [17] used the following protocol  
356 to determine the limits of fusion. The participant had to look at  
357 a 4 cm diameter donut. They increased the horizontal parallax  
358 between stereoscopic images “in the crossed (out of the screen)  
359 or uncrossed (into the screen) directions” until the viewer lost  
360 stereoscopic fusion, or they decreased it until he could fuse im-  
361 ages. Each measurement was realized at least three times. The  
362 results revealed a great inter-participant variability, and suggest  
363 that the depth range increases with an extended exposure to  
364 stereoscopic systems.

365 As seen in Sec. 2.2, other research suggest that a DOF  
366 blur can increase the fusion range, most likely because it  
367 removes high spatial frequencies and might alleviate the  
368 accommodation-vergence conflict, which both have a negative  
369 effect on the limits of fusion.

### 370 2.4.3. Vergence Angle

371 Duchowski et al. [12] stated that stereoscopic stimuli  
372 induce ocular responses similar to those caused by a real scene.  
373 However, they did not quantify the similarity, and instead  
374 shifted the experimental data to match the expected values. We  
375 assume that the correlation rate between ocular movements  
376 caused by real and virtual stimuli, especially vergence angles,  
377 can be used to objectively measure the performance of the con-  
378 figurations. We thus designed a test to monitor eye movements

379 while the participant looks at a real scene or at its reproduction  
380 in VR. This allows us to measure the similarity between virtual  
381 and real stimuli, as well as to compare the realism of virtual  
382 configurations in an innovative way.

383  
384 In conclusion, many research works focused on the qual-  
385 ity of the immersion provided by immersive VR environments.  
386 They covered the impact of ICD and DOF blur. In this paper,  
387 we introduce an approach that combines POR-contingent ICD  
388 and DOF blur. Based on a comparison among various methods  
389 to determine the POR, we come up with a solution involving a  
390 mixture of calibration and lines of sight intersection. We then  
391 evaluated our approach by conducting an experiment based on  
392 several comparative criteria, including an innovative one that  
393 confronts VR and reality.

## 394 3. Methodology

### 395 3.1. Apparatus

396 We conducted our experiment in an iCUBE-4 of  
397 3.1 m × 2.4 m × 2.4 m with projection on the three walls and  
398 the ground. The eight projectors, two per screen, display at a  
399 resolution of 1280 px × 720 px and a frame rate of 120 Hz.

400 The optical head tracking system (OptiTrack) relies on eight  
401 infrared cameras that capture the reflection of infrared lights  
402 over markers placed on any monitored object. This system’s  
403 specifications indicate a submillimeter precision and a latency  
404 of 8.3 ms. Positions and orientations are transmitted by a VRPN  
405 server to the software that controls the projections (MiddleVR)  
406 and to our own software, which uses the collected tracking  
407 data for the real-time update of the virtual cameras’ parame-  
408 ters. The binocular eye tracking is performed by the Eye Track-  
409 ing Glasses (ETG) 2.0 designed by SMI. This device includes  
410 two cameras operating at 60 Hz, located in the spectacle frame  
411 and directed towards the eyes. The ETG are USB connected  
412 and provided along with iViewETG software responsible for  
413 image processing. It operates using a sophisticated model of ocu-  
414 lar behavior based on the method of center-corneal reflections  
415 (PCCR) cited in Sec. 2.3, and behaves as a server transmitting  
416 the ocular tracking data. The ETG provides four 3D vectors in  
417 local coordinates: two sight base points, which correspond to  
418 the center of the eyeballs, and two sight directions which con-  
419 nect base points to the centers of the pupils. The specifications  
420 indicate an accuracy of 0.5° within depth boundaries (40 cm -  
421 infinity) and a range of 80° horizontally and 60° vertically. The  
422 ETG are combined with Volfoni active stereoscopic glasses (see  
423 Fig. 4). Remarks about the number of frames per second (FPS),  
424 and thus the latency of the whole system, are given in Sec. 4.4.

### 425 3.1.1. Calibration

426 The server software supplied with the ETG, iViewETG, al-  
427 lowed us to perform either a 1-point or a 3-point calibration.  
428 They consisted in asking the participant to gaze at either one or  
429 three points in their visual field, while the experimenter clicks  
430 in iViewETG on these same points, on the image filmed by the  
431 scene camera located in front of the ETG at the nose bridge





Figure 4: Eye Tracking Glasses combined with Volfoni active stereoscopic glasses. The markers are placed on the ETG so that head's and ETG's reference frames match, allowing us to collect sight directions in local (ETG) and global (CAVE room) coordinate systems

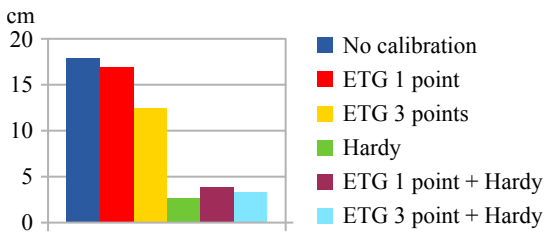


Figure 5: Average distance error obtained with different types of calibration during preliminary tests performed on one participant, for targets at 2 m

level. We chose not to use these options, both because the imprecision results are slightly higher with them (see Fig. 5), and because using it requires a manipulation of the active stereoscopic glasses part in our glasses assembly. During this operation, if the glasses move with respect to the viewer's head, or if the tracking markers are shifted, the imprecision increases.

We thus carried out another type of calibration during the experimentation, based on Hardy's Multiquadric [33], with a rectilinear grid of nine markers. After we set up the ETG on the head, the calibration was achieved by asking the participant to stare successively at nine markers placed on a virtual rectilinear grid and displayed in a random order. The imprecision measurements were carried out on a 25-marker rectilinear grid, and corresponded to the average distance between each computed POR and the current marker during a 2 s recording.

Results revealed an error of 6.47 cm on average for all the participants for targets at 2 m, corresponding to a  $1.85^\circ$  visual angle. Although the specifications of the ETG indicate that it works identically with contact lenses, a one-way ANOVA test showed that wearing lenses leads to a significantly higher POR imprecision ( $F=13.43$ ,  $p=0.002$ ).

### 3.1.2. 3D POR Determination

Preliminary tests performed on one participant included trials to determine the POR by intersecting the lines of sight, as described in Sec. 2.3.2. Yet, because the y-coordinate often diverges slightly in the sight direction vectors given by the ETG, this intersection usually appeared to be at the center of the eyes.

Moreover, other errors and noise present in the measurements led to poor accuracy. Thus, we decided to intersect the lines of sight with the scene and to consider that the POR is located at the intersection, as described in Sec. 2.3.3. Given that the ETG provides binocular data, we tested four ways to determine the POR:

- (1) using the left sight direction only (starting at the left base point), and correcting it with calibration;
- (2) using the right sight direction only (starting at the right base point), and correcting it with calibration;
- (3) using the average of the left and right directions before calibration (starting at the center of the base points), and correcting it with calibration;
- (4) using the average of the corrected left and right directions (starting at the center of the base points).

The results of imprecision tests showed that better results were achieved using method (3), with respective average distance errors of 5.0 cm, 2.7 cm, 2.6 cm, and 3.1 cm. Furthermore, the average distance between each pair of the four PORs, obtained independently from the two sight directions, can be used as a measure of the estimation reliability: the smaller this distance, the smaller the uncertainty of our POR estimation, as it implies that binocular measurements agree with one another.

Due to the noise and jittering observed in the data collected, in particular the fact that some vectors were occasionally directed backwards, we tested two techniques of smoothing, one by averaging through several images (five and ten) the successive positions of the POR, the other using the Unity Smooth-Damp method. Both of these techniques resulted in perceived latency for the authors in the monitoring of the POR, which was inconvenient for the real-time adjustments performed, that must fit the quick phenomenons of saccades and eyes accommodation. Indeed, saccades are performed at a rate of three to five times per second [34], the travel time of the eye being about 10 ms to 100 ms [35]. We thus decided, contrary to some related works [19][26], to keep the data noisy but reactive, and to adapt as quickly as permitted by the tracking systems the variable ICD and DOF blur.

### 3.2. Participants

Eighteen individuals (15 male and 3 female), between the ages of 22 and 49 (average 28), volunteered to participate in our experiment. Five of them wore contact lenses. They all had a significant experience with 3D or virtual reality, having seen at least four 3D films (maximum of 30, average of 11) and 14 of them having played video games (8.6 h/week on average). They all indicated that they usually had no difficulties perceiving depth at movie theatres. Each participant filled out a short pretest questionnaire, providing among other things the aforementioned demographic information and immersion tendency.

Blur \ ICD	Anatomical	Fixed	Variable
Without	B-AICD	B-FICD	B-VICD
With	B+AICD	B+FICD	B+VICD

Table 1: The six configurations tested during the experiment



Figure 6: Absence (left) and presence (right) of the DOF blur used for the experiment

### 508 3.3. Procedure

509 As seen in the literature review, the ICD parameter strongly  
510 impacts the visual comfort and depth perception, thus the whole  
511 performance of a configuration. We decided to test three dif-  
512 ferent approaches for this parameter: the anatomical IPD of  
513 each participant (AICD) measured by the ETG, a fixed single  
514 ICD value chosen by the participant (FICD), or a variable ICD  
515 that is dynamically linearly interpolated between three values  
516 (VICD). These three values correspond to ICDs chosen by the  
517 participant during the start-up phase for three predefined POR  
518 depths (0.4 m for VICD-Near, 1 m for VICD-Middle, and 2.5 m  
519 for VICD-Far). In order to avoid reaching aberrant values, we  
520 keep the ICD constant when the depth of the POR is inferior to  
521 0.4 m or superior to 2.5 m. Regarding the DOF blur, we used  
522 the Depth of Field Scatter of Unity [36] shown in Fig. 6. We  
523 used the parameter “Focus on Transform” that automatically  
524 determines the focal distance using a target object in the scene.  
525 We defined as target a transparent sphere that follows the POR.  
526 We selected the blur intensity value based on our own feeling  
527 of a realistic DOF blur and those of one participant during a  
528 preliminary test. Only one blur intensity was tested to keep a  
529 reasonable number of configurations, thus limiting the duration  
530 of the experiment. The six tested configurations varied in ICD  
531 value and DOF blur presence. Their names are summarized in  
532 Table 1 for the rest of the paper.

#### 533 3.3.1. Start-up

534 The experiment comported a first phase to perform the cal-  
535 ibration based on a virtual grid of nine markers, as described  
536 in Sec. 3.1.1. This calibration was carried out for each partic-  
537 ipant in order to adapt the correction of the vectors to his  
538 anatomical characteristics. Then, the participant had to manu-  
539 ally tune the ICDs that would be used later for FICD and VICD,



Figure 7: Scene used during the experiment

540 with objects displayed at three predefined distances (0.4 m for  
541 VICD-Near, 1 m for FICD and VICD-Middle, and 2.5 m for  
542 VICD-Far). Using a mouse wheel, he could move closer (until  
543 reaching the monoscopic configuration) or move apart (with-  
544 out limits) the two virtual cameras, until reaching a satisfactory  
545 value considering his visual comfort and depth perception. For  
546 this last criterion, we indicated the objects’ distances using a  
547 tape measure, which allowed the participant to ascertain that  
548 his perception matched the actual size and distance. He could  
549 also use the general depth cues given by the other objects of the  
550 scene (see Fig. 7) in order to confirm his choice. Every choice  
551 was performed three times for each predefined distance, and  
552 averaged to set the final ICD value.

553 Each phase of the experiment described below is linked to  
554 a comparative criterion, and required participants to perform  
555 specific tasks. The start-up lasted around 18 min on average,  
556 followed by 15 min of navigation (including the time to rate),  
557 14 min to determine the limits of fusion, and 11 min for the  
558 vergence comparison phase, for a total duration of 57 min on  
559 average. The order of presentation of the configurations fol-  
560 lowed a Latin square rotation, in order to avoid habituation or  
561 visual fatigue bias.

#### 562 3.3.2. Navigation

563 This phase aimed at evaluating the configurations based on  
564 subjective criteria. It consisted in navigating in a virtual scene  
565 along a predefined path, then rating the configurations accord-  
566 ing to one’s impressions. We defined a fixed 90 s navigation  
567 path in the scene with a dual objective: (1) to show objects of  
568 interest with a wide depth range, and (2) to reduce the variabil-  
569 ity inter- and intra-participant, with the only remaining differ-  
570 ences between the six navigations being the current configura-  
571 tion and the gaze path. After each navigation, the participant  
572 was invited to give grades in five criteria: (1) visual comfort,  
573 (2) rendering realism, (3) fun, (4) depth and distance percep-  
574 tion, and (5) sense of immersion. The continuous rating scale  
575 ranged from “very negative” to “very positive”, as presented in  
576 Sec. 2.4.1.

#### 577 3.3.3. Limits of Fusion

578 This phase of the experiment was designed to determine the  
579 viewer’s limits of fusion with each configuration, thereby ob-  
580 taining an objective indication of their effectiveness in terms

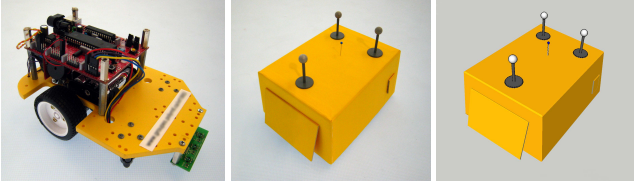


Figure 8: Real and virtual robots

581 of merging near virtual objects. Limits of stereoscopic fusion  
 582 were determined as in [17] with two scenarios: increasing and  
 583 decreasing disparity. For the first one, objects were placed at  
 584 40 cm, a distance that allowed all the participants to fuse the  
 585 images. Using a wireless mouse, the viewer had to bring the  
 586 objects closer until experiencing diplopia. In the second case,  
 587 objects were initially placed extremely close to the participant,  
 588 at 7 cm, and he had to move them away until fusing the im-  
 589 ages. These two scenarios were repeated three times for each  
 590 configuration and averaged to obtain the limit. As this phase  
 591 was prone to induce eye fatigue, the participant was allowed to  
 592 pause for a few seconds between each measure.

### 593 3.3.4. Vergence Comparison

594 In addition to the participant’s subjective assessment of the  
 595 realism of the distances, his ocular behavior, and in particu-  
 596 lar the vergence movements, give objective indications on his  
 597 perception of 3D. These movements naturally accompany the  
 598 inspection of a real scene when the POR changes from a depth  
 599 to another. In the virtual case, the computation of the stereo-  
 600 scopic images or their display may imply a space deformation,  
 601 leading to under- or over-evaluation of the distance that will  
 602 affect the angle of vergence. On the contrary, if the depth in-  
 603 formation is well rendered, the binocular vergence movements  
 604 should reproduce those that would have been performed with  
 605 an identical real scene. Thus, the goal of this last phase was  
 606 to compare the six configurations on the ocular behavior they  
 607 induce when staring at a 3D moving target, using a real mov-  
 608 ing target as a reference. To ensure that the POR follows the  
 609 same path, we guided the participant’s eyes using “identical”  
 610 stimulus. We used a robot capable of following a line on a ta-  
 611 ble. A box overhung the robot, and was topped with a very  
 612 small target that the participant was required to follow during  
 613 the entire course (see Fig. 8). In order to reproduce the robot’s  
 614 movements, the position and orientation of the real robot were  
 615 tracked, saved, and interpolated for moving the virtual robot,  
 616 requiring the “real configuration” to be performed first. As the  
 617 robot’s path can slightly change between each tour, because of  
 618 its groping search in real time of the trace with the aid of detec-  
 619 tors, the recording is done for every participant. The detailed  
 620 setups are shown on Fig. 9.

## 621 4. Results and Discussion

### 622 4.1. Subjective Ratings

623 Fig. 10 summarizes the ratings assigned to each configura-  
 624 tion during the navigation phase. At first glance, it appears that

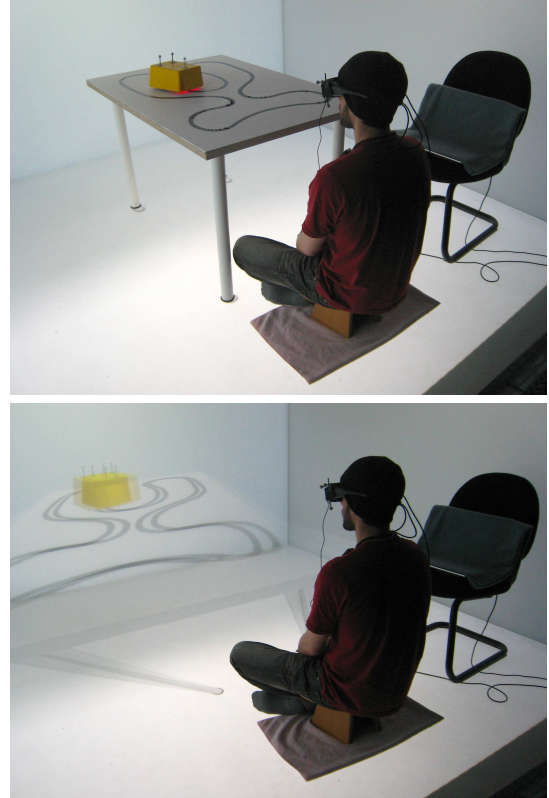


Figure 9: Real and virtual setups for the vergence comparison phase

625 none of the configurations stood out positively in every crite-  
 626 rion: B+AICD presents a better median for comfort and im-  
 627 mersion, B-AICD for realism and fun, and B-FICD for depth  
 628 and distance perception. However, we can note that B+FICD  
 629 always got the lowest medians. We carried out ANOVA tests  
 630 (one-way and two-way) in order to outline statistical impacts of  
 631 the configuration, the ICD value and the presence of DOF blur  
 632 on the results. They did not reveal significant effects, except  
 633 for the blur, which worsened the depth and distance perception  
 634 ( $F=4.91, p=0.034$ ). We can however highlight some interesting  
 635 observations.

636 Regarding the ICD parameter, we note that the order  
 637  $AICD \geq VICD \geq FICD$  occurs in 8 cases out of 10, which  
 638 suggests that AICD was preferred. In addition, we found  
 639 the AICD/FICD ratio to be significantly related to the results  
 640 obtained by the B-FICD configuration in the comfort, fun,  
 641 and depth and distance perception criteria ( $p=0.002, p=0.012,$   
 642  $p=0.040$  as respective correlation probabilities with linear re-  
 643 gressions), with an FICD close to the anatomical one being pre-  
 644 ferred.

645 Concerning the DOF blur, we note that the configuration  
 646 without blur was preferred over its counterpart in 12 cases out  
 647 of 15, showing as in several earlier attempts [5][26][11][28]  
 648 that the participants disliked the addition of a DOF blur. In  
 649 an attempt to explain this trend, and the significant negative  
 650 effect on the depth and distance perception criterion, we per-  
 651 formed an in-depth study of visual inspection. Extracting sac-  
 652 cades and fixations revealed that the fixations were significantly



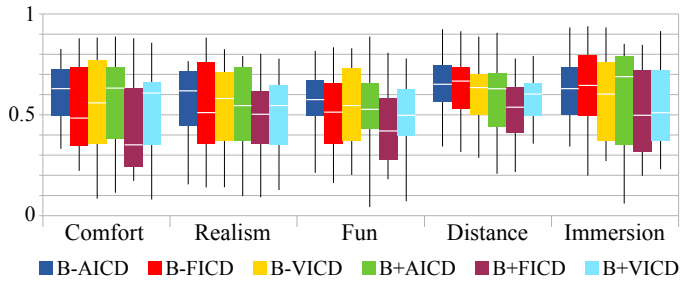


Figure 10: Ratings on the five criteria obtained by each configuration, from “very negative” (0) to “very positive” (1). The rectangle is delimited by the first and third quartiles, and the white line shows the median

fewer ( $F=25.5$ ,  $p<0.01$ ) and longer ( $F=16.9$ ,  $p<0.01$ ) with blurred configurations. The saccades also lasted longer ( $F=236$ ,  $p<0.01$ ), but their average angular distances were not significantly different ( $F=1.02$ ,  $p=0.316$ ), which supports the idea of a slowdown in the visual inspection of the scene. The average number of inspected objects also significantly decreased ( $F=12.2$ ,  $p<0.01$ ). It appeared that during our experiment, the average number of FPS was different between the blurred (9.4 FPS) and non-blurred (13.0 FPS) configurations. We assume that the participants noticed the lag and adapted, consciously or unconsciously, their visual inspection speed to alleviate the delay in parameters update.

In summary, B-AICD obtained higher ratings in general and a higher average rating, although not statistically significant. It suggests that on a subjective basis, the anatomical ICD is preferred and the presence of a DOF blur is detrimental, likely due to the insufficient update speed of the POR-contingent parameters.

Besides, in order to evaluate the accommodation-vergence conflict, we computed the absolute difference between the distances of accommodation and of convergence (see Fig. 1) during the navigation phase. We obtained average distances of 1.30 m for the accommodation, 3.55 m for the convergence, and 2.36 m of absolute difference between them. By comparing the ratings with the absolute difference for each participant, for each configuration, it seems that the accommodation-vergence conflict did not influence the subjective evaluations. We took as statistical measure the distance correlation, which was between 0.20 and 0.27 for the five criteria.

#### 4.2. Limits of Fusion

This phase aimed to compare the ease of stereoscopic fusion allowed by each configuration, by determining the closest fusion distance for every participant. In the results summarized in Fig. 11, we notice that with the configurations using FICD, participants had more difficulties fusing close objects, with the limits being greater. A two-way ANOVA revealed that the ICD parameter indeed had a significant effect (for increasing disparity scenario  $F=3.93$ ,  $p=0.023$ , for decreasing disparity scenario  $F=4.74$ ,  $p=0.011$ ). By comparing B-FICD and B+FICD to all other configurations, we determined that these two were significantly worse in terms of limit of fusion than the others (a paired

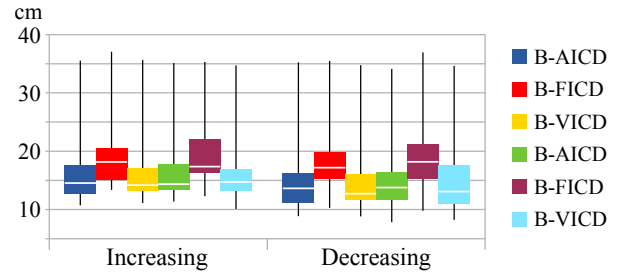


Figure 11: Closest distances of fusion. The average values are 17.11 cm for the increasing scenario, and 16.24 cm for the decreasing one, the limits of fusion per se being located between the results obtained for each scenario

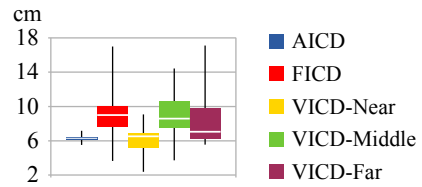


Figure 12: Anatomical ICD, and ICD values chosen during setup. The participants’ AICDs were between 5.51 cm and 7.17 cm (6.28 cm on average), whereas their choices for ICD were between 2.38 cm and 17.11 cm. We note that the chosen values for VICD-Near are close to the AICD’s

t-test gave a  $p$ -value  $<0.01$  for increasing and decreasing scenarios). This can be explained by the fact that FICD is higher than the other ICD values (see Fig. 12), as the configurations using VICD actually use VICD-Near when the POR is located at a depth of under 0.4 m. With a higher ICD, the horizontal disparity between left and right images is more significant, leading to a greater degree of difficulty fusing them. We hence recommend, when scenes with close objects are to be displayed with a fixed ICD, to limit the maximum value allowed for the viewer’s choice.

The DOF blur did not seem to have any influence, contrary to what suggested the literature review [27]. We assume that this is due to the fact that for the limits of fusion reached by most participants, the objects took an important part of the screen, the blurred background thus being a minor portion of the image.

#### 4.3. Visual Behavior Comparison Using a Real Scene

Unlike the two previous criteria, this one relies on a real setup used as a reference to compare the virtual configurations, in order to provide insights on their effective perceptual realism. We took two measurements related to the visual path: (1) the vergence angle and (2) the angular deviation from a target.

The vergence angle is a good indicator of the efficiency of the ICD. Indeed, an inappropriate ICD leads to unrealistic disparities between images, and thus to an under- or over-estimation of the target’s depth by the viewer, which in turn affects his eyes convergence. We considered the global vergence angle, computed directly from the two corrected sight directions, as well as the eyes rotation toward each other by using the angle between the projection of the sight directions on the horizontal plane.

725 The angular deviation from a target refers to the angle be-  
 726 tween the vector from the center of the eyes (center of the sight  
 727 base points) to the POR and the vector from the center of the  
 728 eyes to the target position. Therefore, it reflects the angular distance  
 729 between the location where the participant is looking according  
 730 to our calculations (the POR), and the location where he is actually  
 731 looking (the target). This angular deviation is thus an indicator of  
 732 the accuracies of: the tracking systems, the calculations used to  
 733 correct the sight direction vectors and to compute the POR, and  
 734 finally the geometry rendering with the virtual configuration. Similarly  
 735 to the vergence, we considered the angular deviation as well as its  
 736 horizontal projection.

737 The more these two measurements reproduce the ones recorded  
 738 in the real case, the more the virtual configuration can be considered  
 739 realistic, as it induced a realistic depth perception whatever the  
 740 difference between the ICD and the viewer's anatomical IPD. Regarding  
 741 the deformation inherent to the CAVE, as it was identical for all  
 742 the configurations, we assume the results differences can only be  
 743 attributed to the ICD values and the presence of DOF blur.

744 Before performing the analysis, vergence and angular data were  
 745 manually processed to remove outliers produced by eye tracking.  
 746 Indeed, when infrared reflections cannot be reliably detected and  
 747 tracked for the PCCR, for example due to eye-lashes or blinks [37],  
 748 the ETG deliver invalid values for positions and sight direction  
 749 vectors. Right before or after these periods, we observe brief peaks  
 750 with amplitudes too high to correspond to vergence movements,  
 751 which we attribute to the fact that only some diodes were reflected,  
 752 the rest being hidden by the eyelid. We manually removed these  
 753 peaks, thus replacing them by a linear interpolation between the  
 754 previous and next reasonable values.

#### 757 4.3.1. Vergence Comparison

758 Fig. 13 shows, for a representative participant, the curves of his  
 759 vergence angle as a function of time for the real and virtual  
 760 configurations. The robot performed two laps, passing closer to  
 761 the participant around times 15 s and 55 s. The distance between  
 762 the robot and the participant is also plotted on Fig. 13. We observe  
 763 that the variations were similar for the real and virtual cases,  
 764 thus demonstrating, as noticed in the literature review, that  
 765 stereoscopic images induce realistic ocular movements. Compared  
 766 to previous works, gathering data for the real case allows us to  
 767 make deeper qualitative and quantitative observations. For example,  
 768 considering the general shape of the curve, we note that on  
 769 average the vergence angle variations had a smaller amplitude  
 770 in the virtual case (this is particularly visible during the first  
 771 10 s of Fig. 13 (bottom)).

772 As for the quantitative comparison, for each of the virtual  
 773 configurations, we computed the average distance between its  
 774 curve and the one obtained in the real case (see Fig. 14). ANOVA  
 775 tests (one-way and two-way) revealed no significant effect of the  
 776 configuration, the ICD value or the presence of DOF blur. However,  
 777 we note that based on the median, the most realistic configuration  
 778 is B-AICD, followed by B+AICD when considering the global  
 779 vergence, and by B+VICD when considering the horizontal  
 780 vergence.

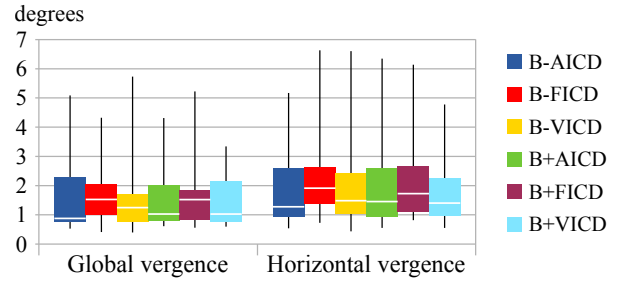


Figure 14: Average distances of global and horizontal vergence angles observed in the virtual cases with respect to the real one

781 Regarding the ICD parameter, AICD and VICD performed  
 782 similarly, although AICD obtained vergence angles slightly  
 783 closer to those measured during the real case. This is likely attributed  
 784 to the large range of values taken by VICD during this phase. Indeed,  
 785 as the distance between the robot and the participant took values on  
 786 average from 0.37 m to 1.24 m, VICD varied mainly between  
 787 VICD-Near et VICD-Middle, which, as shown on Fig. 12, was close  
 788 to FICD and even higher than VICD-Far. Besides, B-FICD and  
 789 B+FICD, which shared the same ICD value, led to greater differences  
 790 of vergence angle, and a paired t-test revealed that these configurations  
 791 were significantly further from the real configuration when considering  
 792 horizontal vergence ( $p=0.0257$ ). As for the limits of fusion  
 793 criterion, this result can be attributed to the FICD higher values  
 794 that lead, for close objects, to great disparities which triggered  
 795 ocular behavior far from those witnessed in the real case.

796 The presence of DOF blur did not seem to have an influence on  
 797 the configurations' performance. We observed that adding blur led  
 798 to worse results when combined with AICD and better ones with  
 799 VICD, in a non-significant way.

800 We also computed the relative deviations, which better reflect  
 801 the significance of the distance between the curves, by dividing  
 802 the vergence distances with the average vergence angles measured  
 803 during the real case (see Table 2). These rates confirm the previous  
 804 results, AICD and VICD obtaining similar lower deviation from  
 805 the real case than FICD, and the presence or absence of DOF blur  
 806 not showing any influence. We note that, although the vergence  
 807 angle followed the same variations in both virtual and real cases,  
 808 the differences in amplitude led to a relative deviation of up to  
 809 38.5% (and 71.8% horizontally) with respect to the real case.  
 810 With regard to these high deviations, it has to be taken into  
 811 account that the average global vergence angle for the real  
 812 configuration was of  $5.1^\circ$ . Thus, the higher relative deviation  
 813 corresponds to  $2.0^\circ$ , which is similar to the inaccuracy of  
 814  $1.85^\circ$  measured after the calibration phase.

#### 816 4.3.2. Angular Deviation from a Target

817 Fig. 15 presents, for a representative participant, the curves of  
 818 the horizontal angular deviation as a function of time, for the real  
 819 and averaged virtual configurations. We first observe that the  
 820 angular deviation was around zero degree for the real configuration,  
 821 indicating that the POR direction we computed coincided with the  
 822 vector between the eyes and the position of the target monitored  
 823 by the tracking system. The angular devi-

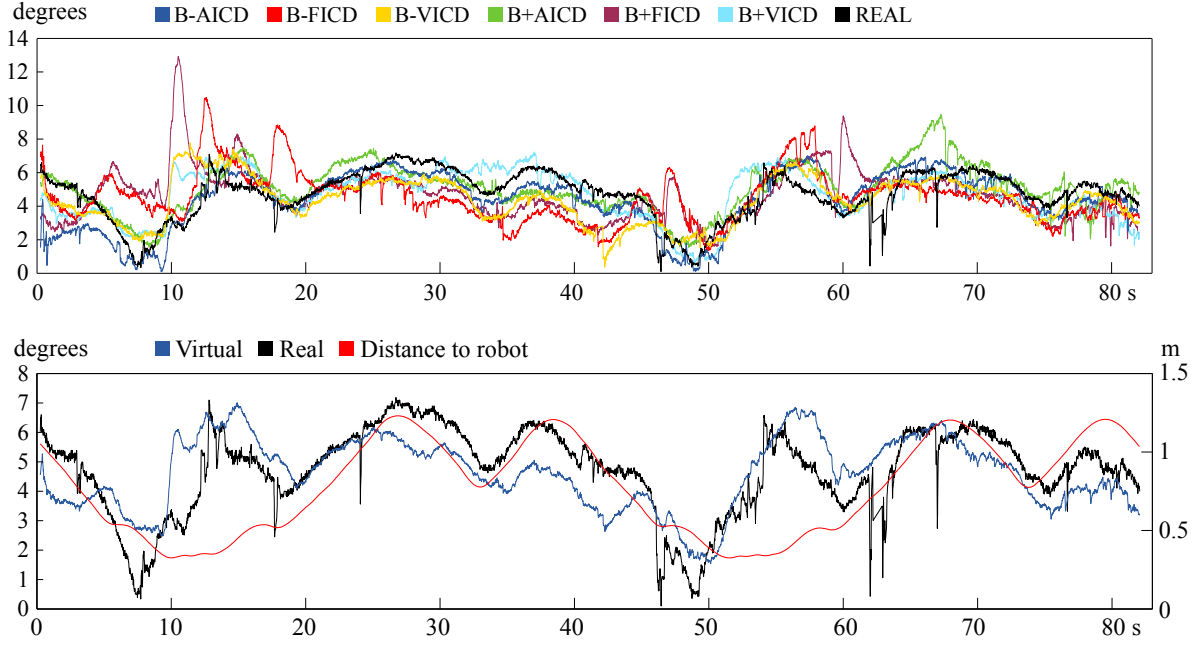


Figure 13: (Top and bottom) Global vergence angle measured for real and virtual configurations for a representative participant. In the bottom, the curves for the six virtual configurations were averaged in order to highlight more clearly the difference of vergence angle between the virtual and real cases, and put in parallel with the distance to the robot

	Global Vergence	Horizontal vergence
B-AICD	31.5%	51.2%
B-FICD	38.5%	71.8%
B-VICD	36.0%	60.6%
B+AICD	32.3%	53.9%
B+FICD	36.5%	67.7%
B+VICD	31.9%	57.6%

Table 2: Relative deviation with the average global and horizontal vergence angles measured during the real case

824 ation was greater in the virtual cases, which indicates that the  
825 robot’s position in the CAVE coordinates (where the viewer saw  
826 it) was not the same as its position in the virtual world coordi-  
827 nates. This corresponds to a deformation of space coordinates,  
828 probably not only due to the stereoscopic parameters of the con-  
829 figurations but also to the display calibration. While being a  
830 limitation in quantifying the absolute realism of a given config-  
831 uration, the deformation induced by the CAVE setup should not  
832 impact the configuration results relative to each other, since it  
833 remains the same during the experiment.

834 Fig. 16 summarizes, for each configuration, the distance be-  
835 tween the angular deviations from the target compared to those  
836 obtained with the real configuration. ANOVA tests (one-way  
837 and two-way) revealed that the configuration, the ICD value, or  
838 the presence of DOF blur did not have a statistically significant  
839 impact. However, we note that the configurations obtaining the  
840 lowest median, i.e. the smallest distance with respect to the real  
841 case, were B-VICD, followed by B+FICD. When considering  
842 the horizontal angular deviation, B-FICD had the smallest med-  
843 ian, followed by B+VICD. It is worth noting that the FICD

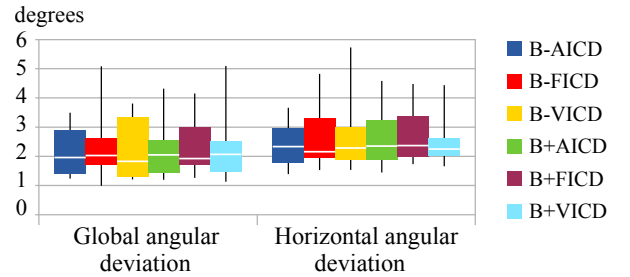


Figure 16: Average distances of global and horizontal angular deviations observed in the virtual cases with respect to the real one. **N.B.** These results do not include one of the participants, for whom measurements showed large errors (an angular deviation greater than  $120^\circ$  over 50% of the time with the real and B-VICD configurations)

844 performed similarly to the others ICD values for this criterion.  
845 High stereoscopic disparities therefore seem to only influence  
846 the vergence angle and not the gaze direction.

#### 847 4.4. Remarks and Future Work

848 As can be observed in the results, none of the configurations  
849 stood out significantly from the others as being most effective,  
850 implying that the benefits of a variable ICD or the presence of  
851 a DOF blur are hard to grasp. As in previous works with DOF  
852 blur [28][26] presented in Sec. 2.2, we assume that the delay in  
853 the adjustment of these POR-contingent parameters, followed  
854 by the images update, must have been perceivable by the par-  
855 ticipants and detrimental to such adjustments. Indeed, although  
856 we did not compute the total latency, which takes into account  
857 all the tracking systems’ latency, we measured the number of  
858 FPS which gives an indication of the maximum system reactiv-  
859 ity. As given in Sec. 4.1, the average FPS during the navigation

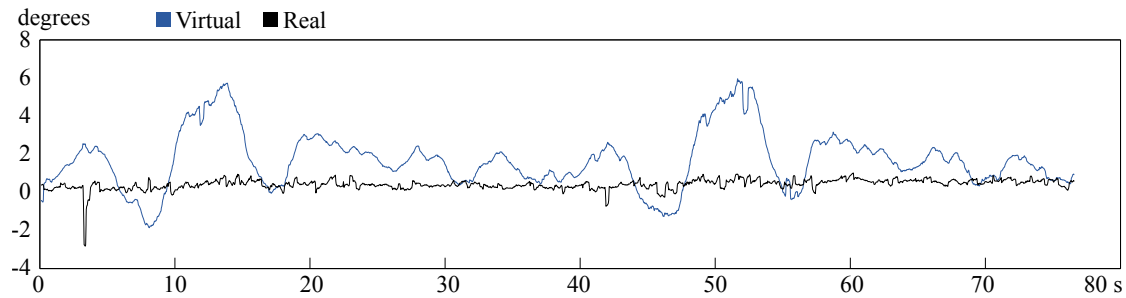


Figure 15: Horizontal angular deviation from a target measured for the real and averaged virtual configurations

860 phase was 13.0 FPS without DOF blur and 9.4 FPS with it. It is  
 861 likely that such performance affected the user subjective appreci-  
 862 ations, although none of them reported VR sickness. How-  
 863 ever, while being a limitation to the significance of the results  
 864 regarding the perceptual realism of the configurations, we as-  
 865 sume their relative comparison is still relevant. The number of  
 866 FPS was almost the same during the limits of fusion determina-  
 867 tion (12.8 FPS in average), which we attribute to the geometrical  
 868 complexity of the scene used during these two phases of the  
 869 experiment. On the other hand, we reached 35.1 FPS in aver-  
 870 age during the visual behavior comparison thanks to the robot  
 871 scene, thus probably lowering the impact of the update time.

872 In order to further investigate the adjustment of stereoscopic  
 873 parameters, other values for variable ICD and blur intensity  
 874 could be tested. First, if the setup requires a fixed ICD, the poor  
 875 results obtained by B-FICD and B+FICD would suggest that  
 876 the participant not be allowed to select this value, but rather to  
 877 compare a set of predefined ICDs and select the top performer.  
 878 If a dynamic adjustment is allowed, a similar test to the one  
 879 used to compare visual behaviors, i.e. reproducing a real scene  
 880 in VR, can also be used to determine the optimum ICD values.  
 881 Indeed, after recording the viewer's vergence angles in the real  
 882 case, the ICD would be modified in real time while the partic-  
 883 ipant observes the virtual scene until his vergence angles are  
 884 identical to those recorded. A neural network would be trained  
 885 with such a procedure in order to determine the best ICD values  
 886 during the real experiment.

887 Concerning the DOF blur, only one intensity was tested in  
 888 order to keep a reasonable number of configurations and thus  
 889 experiment duration. However, some research suggest that in-  
 890 dividual tuning is needed to find the appropriate value [5][11],  
 891 which could also vary according to the accommodation dis-  
 892 tance. Moreover, several blur algorithms could be evaluated  
 893 on how closely they replicate the natural viewing blur, using  
 894 for instance similar methods to the ones proposed for the ICD.

## 895 5. Conclusion

896 This project was originated from a desire to measure and  
 897 improve the effectiveness of stereoscopic rendering in a VR en-  
 898 vironment, particularly with respect to the visual comfort dur-  
 899 ing extended exposure, the perceptual realism and the feeling  
 900 of presence. Our experiment compared six configurations, dif-  
 901 ferent in their ICD values (anatomical, fixed or variable) and

902 the presence or absence of a DOF blur, two parameters known  
 903 for their influence on the criteria cited above. The variable ICD  
 904 and the DOF blur relied on the viewer's POR in order to be  
 905 adjusted in real time. For the ICD, the goal was to adapt the  
 906 amount of disparity, which influence the sense of depth, ac-  
 907 cording to the depth level on which the viewer chooses to focus.  
 908 The blur aimed to reproduce the DOF blur that occurs in natu-  
 909 ral vision. Results showed that VICD and AICD were similarly  
 910 efficient regarding each phase of the experiment. In particular,  
 911 B-AICD and B+VICD led to more realistic vergence angles,  
 912 and B-VICD obtained the smallest distance to the real angu-  
 913 lar deviations from a target (considering the medians). On the  
 914 other hand, the FICD led to significantly higher fusion diffi-  
 915 culties, and to greater differences of horizontal vergence angles  
 916 as compared to those measured in the real case. The subjec-  
 917 tive ratings revealed that an FICD closer to the AICD led to  
 918 higher ratings. The presence of DOF blur did not significantly  
 919 impact the ability of fusion or the similarity of ocular behavior  
 920 between real and virtual. On the other hand, the participants  
 921 expressed a dislike in their subjective ratings towards blurred  
 922 configurations, which was significant in the depth and distance  
 923 perception criterion. This experiment highlighted the difficulty  
 924 of obtaining benefits from varying the ICD or adding a DOF  
 925 blur, even though the technical limitations encountered and de-  
 926 scribed in Sec. 4.4 may have counteracted the advantages of  
 927 these real-time adjustments of parameters based on the POR.

928 As part of this project, we also designed an innovative  
 929 methodological framework to objectively compare the stereo-  
 930 scopic configurations. The test is based on a recording of the  
 931 viewer's eye movements while he stares at real and virtual mov-  
 932 ing targets. The comparison between ocular behaviors, particu-  
 933 larly the vergence angle, provides an interesting and quantifi-  
 934 able measure of the perceptual realism and the geometry render-  
 935 ing. It could be used in the future as an evaluation criterion: a  
 936 greater correlation between the eye responses with the real and  
 937 virtual configurations indicates an improved perceptual realism  
 938 of the depth rendering. It can also be used to find the optimum  
 939 stereoscopic parameters, by modifying them until the vergence  
 940 corresponds to that measured in the real case.

941 This comparison method would be a step forward to insure  
 942 the correspondence between visual behavior in real and virtual  
 943 setups, and might help increase the feeling of immersion. This  
 944 is of particular interest to research in psychiatry, when tracking  
 945 gaze behavior is used as source of diagnosis [2][1][3]. More-



- over, in this context, the POR recording provides additional tools for the clinician, such as visual paths, hit maps, measurements of fixations and saccades, which can help in the interpretation of the visual behavior in terms of attention.
- [1] Renaud P, Rouleau JL, Granger L, Barsetti I, Bouchard S. Measuring sexual preferences in virtual reality: A pilot study. *CyberPsychology & Behavior* 2002;5(1):1–9.
  - [2] Renaud P, Chartier S, Rouleau JL, Proulx J, Trottier D, Bradford JP, et al. Gaze behavior nonlinear dynamics assessed in virtual immersion as a diagnostic index of sexual deviancy: preliminary results. *Journal of Virtual Reality and Broadcasting* 2009;6(3).
  - [3] Renaud P, Bouchard S, Proulx R. Behavioral avoidance dynamics in the presence of a virtual spider. *Information Technology in Biomedicine, IEEE Transactions on* 2002;6(3):235–43.
  - [4] Hardless G, Meilinger T, Mallot H. Virtual reality and spatial cognition. In: *International Encyclopedia of the Social Behavioral Sciences*. Elsevier Science; 2015, p. 133–7.
  - [5] Vinnikov M, Allison RS. Gaze-contingent depth of field in realistic scenes: The user experience. In: *Proceedings of the Symposium on Eye Tracking Research and Applications*. ACM; 2014, p. 119–26.
  - [6] Moreau G. Visual immersion issues in virtual reality: a survey. In: *Graphics, Patterns and Images Tutorials (SIBGRAPI-T), 2013 26th Conference on*. IEEE; 2013, p. 6–14.
  - [7] Lambooi M, Fortuin M, Heynderickx I, IJsselstein W. Visual discomfort and visual fatigue of stereoscopic displays: a review. *Journal of Imaging Science and Technology* 2009;53(3):30201–1.
  - [8] Rushton SK, Riddell PM. Developing visual systems and exposure to virtual reality and stereo displays: some concerns and speculations about the demands on accommodation and vergence. *Applied Ergonomics* 1999;30(1):69–78.
  - [9] Jones GR, Lee D, Holliman NS, Ezra D. Controlling perceived depth in stereoscopic images. In: *Photonics West 2001-Electronic Imaging*. International Society for Optics and Photonics; 2001, p. 42–53.
  - [10] Milgram P, Krüger M. Adaptation effects in stereo due to on-line changes in camera configuration. In: *SPIE/IS&T 1992 Symposium on Electronic Imaging: Science and Technology*. International Society for Optics and Photonics; 1992, p. 122–34.
  - [11] Hillaire S, Lécuyer A, Cozot R, Casiez G. Depth-of-field blur effects for first-person navigation in virtual environments. *Computer Graphics and Applications, IEEE* 2008;28(6):47–55.
  - [12] Duchowski AT, Pelfrey B, House DH, Wang R. Measuring gaze depth with an eye tracker during stereoscopic display. In: *Proceedings of the ACM SIGGRAPH Symposium on Applied Perception in Graphics and Visualization*. ACM; 2011, p. 15–22.
  - [13] Daugherty BC, Duchowski AT, House DH, Ramasamy C. Measuring vergence over stereoscopic video with a remote eye tracker. In: *Proceedings of the 2010 Symposium on Eye-Tracking Research & Applications*. ACM; 2010, p. 97–100.
  - [14] Wann JP, Rushton S, Mon-Williams M. Natural problems for stereoscopic depth perception in virtual environments. *Vision research* 1995;35(19):2731–6.
  - [15] Allison RS. The camera convergence problem revisited. In: *Electronic Imaging 2004*. International Society for Optics and Photonics; 2004, p. 167–78.
  - [16] Stelmach LB, Tam WJ, Speranza F, Renaud R, Martin T. Improving the visual comfort of stereoscopic images. In: *Electronic Imaging 2003*. International Society for Optics and Photonics; 2003, p. 269–82.
  - [17] Woods AJ, Docherty T, Koch R. Image distortions in stereoscopic video systems. In: *IS&T/SPIE's Symposium on Electronic Imaging: Science and Technology*. International Society for Optics and Photonics; 1993, p. 36–48.
  - [18] Best S. Perceptual and oculomotor implications of interpupillary distance settings on a head-mounted virtual display. In: *Aerospace and Electronics Conference, 1996. NAECON 1996.*, *Proceedings of the IEEE 1996 National*; vol. 1. IEEE; 1996, p. 429–34.
  - [19] Ware C. Dynamic stereo displays. In: *Proceedings of the SIGCHI conference on Human factors in computing systems*. ACM Press/Addison-Wesley Publishing Co.; 1995, p. 310–6.
  - [20] Bennett A, Francis J. The eye as an optical system. *The eye* 1962;4:101–15.
  - [21] Celikkan U, Cimen G, Kevinc EB, Capin T. Attention-aware disparity control in interactive environments. *The Visual Computer* 2013;29(6-8):685–94.
  - [22] Kulshreshth A, LaViola Jr JJ. Dynamic stereoscopic 3d parameter adjustment for enhanced depth discrimination. In: *Proceedings of the 2016 CHI Conference on Human Factors in Computing Systems*. ACM; 2016, p. 177–87.
  - [23] Bernhard M, Dell'mour C, Hecher M, Stavrakis E, Wimmer M. The effects of fast disparity adjustment in gaze-controlled stereoscopic applications. In: *Proceedings of the Symposium on Eye Tracking Research and Applications*. ACM; 2014, p. 111–8.
  - [24] Hillaire S, Lécuyer A, Cozot R, Casiez G. Using an eye-tracking system to improve camera motions and depth-of-field blur effects in virtual environments. In: *Virtual Reality Conference, 2008. VR'08*. IEEE. IEEE; 2008, p. 47–50.
  - [25] Leroy L, Fuchs P, Moreau G. Real-time adaptive blur for reducing eye strain in stereoscopic displays. *ACM Transactions on Applied Perception (TAP)* 2012;9(2).
  - [26] Duchowski AT, House DH, Gestring J, Wang RI, Krejtz K, Krejtz I, et al. Reducing visual discomfort of 3d stereoscopic displays with gaze-contingent depth-of-field. In: *Proceedings of the ACM Symposium on Applied Perception*. ACM; 2014, p. 39–46.
  - [27] Nagata S. The binocular fusion of human vision on stereoscopic displays: field of view and environment effects. *Ergonomics* 1996;39(11):1273–84.
  - [28] Brooker JP, Sharkey PM. Operator performance evaluation of controlled depth of field in a stereographically displayed virtual environment. In: *Photonics West 2001-Electronic Imaging*. International Society for Optics and Photonics; 2001, p. 408–17.
  - [29] Kwon YM, Jeon KW, Ki J, Shahab QM, Jo S, Kim SK. 3D Gaze Estimation and Interaction to Stereo Display. *IJVR* 2006;5(3):41–5.
  - [30] Pfeiffer T. Measuring and visualizing attention in space with 3d attention volumes. In: *Proceedings of the Symposium on Eye Tracking Research and Applications*. ACM; 2012, p. 29–36.
  - [31] Essig K, Pomplun M, Ritter H. A neural network for 3D gaze recording with binocular eye trackers. *The International Journal of Parallel, Emergent and Distributed Systems* 2006;21(2):79–95.
  - [32] Blum T, Wiczorek M, Aichert A, Tibrewal R, Navab N. The effect of out-of-focus blur on visual discomfort when using stereo displays. In: *Mixed and Augmented Reality (ISMAR), 2010 9th IEEE International Symposium on*. IEEE; 2010, p. 13–7.
  - [33] Zachmann G, et al. *Virtual Reality in Assembly Simulation: Collision Detection, Simulation Algorithms, and Interaction Techniques*. Fraunhofer-IRB-Verlag; 2000.
  - [34] Lorenceau J. Cursive writing with smooth pursuit eye movements. *Current Biology* 2012;22(16):1506–9.
  - [35] Shebilske WL, Fisher DF. Understanding extended discourse through the eyes: How and why. In: Groner R, Menz C, Fisher DF, Monty RA, editors. *Eye Movements and Psychological Functions: International Views*. Hillsdale, NJ: Lawrence Erlbaum Associates; 1983, p. 303–14.
  - [36] Unity Manual depth of field. <https://docs.unity3d.com/460/Documentation/Manual/script-DepthOfFieldScatter.html>; 2014. Accessed: 2014.
  - [37] Holmqvist K, Nyström M, Andersson R, Dewhurst R, Jarodzka H, Van de Weijer J. *Eye tracking: A comprehensive guide to methods and measures*. OUP Oxford; 2011.